Project 2 - Task 5: Research and Technical Support for WIPP

Trivalent Actinide and Lanthanide Partitioning in Culebra Dolomite

Date submitted:

May 15, 2017

Principal Investigator:

Leonel E. Lagos, Ph.D., PMP®

Florida International University Collaborator:

Hilary P. Emerson, PhD, EI, Task Manager

Los Alamos National Laboratory Collaborators:

Timothy Dittrich, PhD

Donald Reed, PhD

Submitted to:

U.S. Department of Energy
Office of Environmental Management
Under Cooperative Agreement # DE-EM0000598

FIU | Applied Research Center
FLORIDA INTERNATIONAL UNIVERSITY

Table of Contents

Table of Figures

Table of Tables

1.0 Introduction

There is a need to better understand trivalent actinide and lanthanide sorption processes on carbonate minerals as they are common in the natural environment and play an important role in the fate and transport of actinide elements with respect to natural systems and disposal of radioactive waste in deep geologic repositories. Carbonate minerals may be important in determining the fate of trivalent actinides and lanthanides due to strong complexation with aqueous carbonate released from minerals as well as strong sorption to the minerals themselves (Zavarin et al., 2005). For example, dolomite ($CaMg[CO_3]_2$) is present in the Rustler formation above the Waste Isolation Pilot Plant (WIPP) which disposes of transuranic (TRU) waste near Carlsbad, NM. Moreover, radionuclide partitioning within this formation has been determined to be a key parameter in the performance assessment (Bertram-Howery et al., 1990), likely due to its high transmissivity which may limit brine flow in and out of the WIPP repository if human intrusion occurs after closure (Meigs et al., 1997; Perkins et al., 1999).

The most likely release pathway in the event of human intrusion is through transport in the permeable layers of the Rustler formation located above the Salado formation which contains the WIPP repository. Within the Rustler formation, the Culebra dolomite member is the most transmissive geologic layer and, therefore, the most susceptible release pathway for liquids (Meigs et al., 1997; Perkins et al., 1999). However, the fate of trivalent actinides and lanthanides in this system is still not well understood due to their limited solubility and the narrow range of conditions evaluated in previous work.

Experiments measuring sorption to carbonate minerals are complicated as dissolution and growth occur much more rapidly than for metal (hydr)oxides (Brady et al., 1999). For example, Perkins *et al*. conducted intact-core experiments with Culebra dolomite but did not observe breakthrough of Am(III) after many months of injection (Perkins et al., 1999). In addition to the expected strong sorption of Am(III), it is likely that precipitation near the inlet due to oversaturation of influent solutions limited Am recovery from the core experiments.

Batch-type laboratory experiments have also produced limited datasets describing trivalent actinide and lanthanide sorption to dolomite. Partitioning coefficients (K_ds) reported in the memo by Brush and Storz covered several different brine compositions related to the WIPP but did not report the pH for Am(III) K_ds and reported an incomplete dataset for Nd(III) in the presence of atmospheric CO_2 and 0.05 M NaCl (Brush and Storz, 1996). Moreover, Brady *et al*. used a limited residence time reactor technique but exceeded Nd(III) solubility for pH 6-8 and reported only a limited pH range (3-6) for Am(III) at 0.05 and 0.5 M NaCl with a large uncertainty in ICP-MS analyses due to detection limits (Brady et al., 1999). Overall, the range of K_ds reported for dolomite spans from $10^{3.4}$ to 10^{6} (Brady et al., 1999; Brush and Storz, 1996; Perkins et al., 1999).

Dolomite can be visualized as alternating layers of calcite and magnesite (Reeder and Wenk, 1983). It is expected that the trivalent actinides and lanthanides will interact with carbonate minerals through either adsorption or exchange with surface ions. Because of the similarity in ionic radii for Am^{3+} and Nd^{3+} to Ca^{2+}, it is possible that Nd/Am can exchange with Ca^{2+} on the surface (Brady et al., 1999). However, carbonate minerals do not have a significant ion exchange capacity. TRLFS experiments at pH 8.1 identified two surface species for Cm on calcite: (1) a surface sorbed species, and (2) an incorporated species (Fernandes et al., 2008).

The bulk of the work investigating sorption of trivalent actinides and lanthanides to carbonate minerals has been conducted on calcite minerals (Stout and Carroll, 1993). The extent of adsorption on carbonate mineral surfaces is generally correlated with the rates of dissolution and growth. Chou and team previously reported that dissolution of dolomite occurs much more slowly than calcite (Chou et al., 1989). Therefore, sorption of contaminants is hypothesized to be less on dolomite as compared to calcite.

The limited body of work on sorption to carbonate minerals does not include adequate data at elevated ionic strengths (IS) as expected at the WIPP repository. Applicable brines in the WIPP are on the order of 5.3 M (ERDA-6) and 7.4 M (GWB) (Lucchini et al., 2014), and far-field transport may result in a wide range of lower ionic strengths required for transport models in the performance assessment. Moreover, previous researchers have reported a varying effect of ionic strength on sorption processes of trivalent actinides and lanthanides on various minerals: (1) no effect of IS for 0.005 – 0.5 M Nd/Am sorption to dolomite (Brady et al., 1999; Schnurr et al., 2015), (2) a decrease in sorption with IS for Np sorption to hematite (Powell, 2016), and (3) an

increase in sorption with IS for Np to bacteria (Ams et al., 2013; Powell, 2016). Therefore, there is a need to better understand the effects of ionic strength on trivalent actinide and lanthanide sorption and incorporation processes with dolomite.

Because there is insufficient historical data describing the sorption of trivalent actinides and lanthanides to Culebra dolomite, conservative assumptions were made for the WIPP PA. The final K_ds used for the PA for the WIPP were 20 to 400 mL/g for Pu(III) and Am(III) for deep brines (Brush and Storz, 1996). However, these assumptions are based on reported K_ds for Am(III) and Pu(V) [not Pu(III)] with the aforementioned experimental artifacts. Therefore, it is necessary to accurately measure the partitioning of trivalent actinides and lanthanides in these systems to allow for the most realistic prediction in the event that risk assessment models must be updated, conditions within the WIPP change, or human intrusion leads to a potential release.

2.0 Objectives

The overall objective of this task is to evaluate sorption and desorption parameters for trivalent actinides (Pu and Am) and lanthanides (Nd) to Culebra dolomite in simplified systems at variable IS. This project utilizes both mini column and batch experiments in order to gather the most accurate data without experimental artifacts. These data will be used to bridge the gap between applied and basic experimental work to update the performance assessment models for the five year re-certification of the WIPP.

3.0 Materials and Methods

3.1 Mineral Preparation and Characterization

Before experiments were conducted, Culebra dolomite mineral samples were crushed, cleaned and characterized. First, dolomite rock samples are crushed in an impact mortar and pestle and then washed and sieved. The 355 – 500 µm size fraction was utilized for all batch and column experiments. If finer fractions are used for columns, they will likely clog. Therefore, the 355 – 500 µm size fraction was used for all experiments for consistency.

The following procedure was followed:

1. Lightly crush sample in an impact mortar and pestle

2. Sieve dry solid through No. 45, 100 and 200 size sieve
3. Remove largest size fraction (>500 μm) and re-crush
4. Continue steps and 2 and 3 until all solid has been processed through sieves
5. Rinse all solids with Milli-Q (>18 MΩ) H_2O
6. Dry ~24 hours at 40°C
7. Re-sieve all dry solids

The minerals within the Culebra field samples were identified by a combination of x-ray diffraction (XRD) and scanning electron microscopy with energy dispersive x-ray spectroscopy (SEM-EDS). Bulk surface area was estimated through the Brunauer-Emmett-Teller (BET) method by the Mechanical Engineering Department at Florida International University (Micromeritics TriStar II 3020). Based on triplicate sample analysis, the error on BET measurements is less than 20%.

3.2 Batch Sorption Experiments

3.2.1 Batch Experimental Conditions

Experiments were conducted in triplicate at variable solids loading (Culebra dolomite, $CaMg[CO_3]_2$, 0.5, 1.0 and 5.0 g/L) and pH 8.5 to investigate the loading capacity as well as kinetic and equilibrium partitioning of Nd. Initial experiments were conducted with Nd to simplify the protocols without radiation safety hazards, although future experiments will include Am and Pu(III). Experiments were conducted with variable IS 0.01 – 5 M (NaCl + 3 mM $NaHCO_3$).

Nd was not added to batch stock solutions until the pH had equilibrated (24-48 hours). The initial Nd concentration was 20 ppb. Initial experiments and geochemical modeling were conducted to estimate solubility of Nd within the applicable pH range and a conservative initial concentration was chosen in order to exclude precipitation. Controls were also conducted without the presence of the solid phase (Culebra dolomite) to account for sorption to vial walls and losses during pH adjustment. A buffer of 3 mM $NaHCO_3$ was used to control pH and to keep samples close to the level predicted in equilibrium with atmospheric carbon dioxide at pH 8.5.

Experiments were allowed to equilibrate for 48 hours with sampling at multiple time intervals beginning at 15 minutes. This is expected to be sufficient as previous work has reported equilibrium within thirty seconds for Nd/Am to dolomite (Brady et al., 1999) and with Eu/Sm

sorption to calcite within 24 hours (Zavarin et al., 2005). All samples were analyzed by ICP-MS for Nd. Select samples were analyzed by ICP-OES for both Nd and major cations (i.e. Na, Mg, and Ca) present from IS adjustment and dolomite dissolution.

3.2.2 ICP-MS Analysis

Sample preparation was modified for ICP-MS in high IS samples to keep the total dissolved solids (TDS) below the instrument limit of 0.2% or 2000 mg/L. Table 1 shows the theoretical dilutions required for measurement of variable IS samples by ICP-MS.

The limit of detection (LOD) was estimated based on the following equation:

$$LOD = 3.2x\frac{SE}{m} \quad \text{Eqn. 1}$$

Where SE = standard error as calculated based on a linear regression of the calibration and m=slope of a linear fit of a graph of instrument response (counts) versus the known concentration of the standard. The instrument detection limit (without dilution correction) is approximately 0.02 ppb for both ^{144}Nd and ^{146}Nd.

Table 1: Dilution requirements to remain below 0.2% TDS for ICP-MS at variable ionic strength in NaCl

NaCl (mol/L)	NaCl (mg/L)	Dilution
0.01	584	-
0.1	5844	1:3
1	58443	1:30
5	292214	1:150

3.2.3 pC_{H+} Calculations

At high IS conditions, there is a difference between pH (hydrogen ion activity) and pC_{H+} (hydrogen ion concentration). The pH reading of a glass electrode at elevated IS is not straightforward due to: (1) calibration with low IS buffers, and (2) lack of data for activity coefficients. However, a linear function has been shown to fit the data to predict pH and pC_{H+} and is in agreement with previous data (Borkowski et al., 2009; Rai et al., 1995). In this work, pH and pC_{H+} were determined using corrections based on equation 2 as developed previously (Borkowski et al., 2009). Borkowski measured the K-value correction for 5 M NaCl as 0.82 ± 0.03. The linear equation is

shown in equation 3, where K=correction factor and IS represents the total IS in mol/L. Although Rai *et al.* (1995) did not develop a linear correlation for the K-value, they did measure this factor at variable IS in NaCl solutions and it correlates well with the equation developed by Borkowski (2009).

$$pC_{H^+} = pH + K \quad \text{Eqn. 2}$$

$$K = [IS \times -0.1868 \pm 0.0082] + 0.073 \quad \text{Eqn. 3}$$

3.2.4 Partitioning Coefficient and Kinetics Calculations

Equilibrium partitioning coefficients (K_ds) were calculated per eqns. 1 and 2 below. Kinetic parameters were also estimated based on the equations outlined in

Table 2. However, additional kinetic models will be examined in future work. Because three solids loadings were considered for each IS condition, Freundlich and Langmuir isotherms will also be fit for experimental data in the future (Table 3).

$$[An]_{min} = \frac{([An]_{aq,i} - [An]_{aq,t})V_L}{m_{min}} \quad \text{Eqn. 4}$$

where: $[An]_{min}$= total concentration in mineral, ppb (μg/kg$_{min}$)

$[An]_{aq,i}$= initial total aqueous concentration, ppb (μg/L)

$[An]_{aq,t}$= total aqueous concentration at time, t, ppb (μg/L)

V_L= sample liquid volume, L

M_{min}= sample mineral mass, kg$_{min}$

The sediment water partitioning coefficient, K_d, will be calculated using the following equation:

$$K_d = \frac{[An]_{min}}{[An]_{aq}} \quad \text{Eqn. 5}$$

Table 2: Kinetic model equations for batch sorption experiments

Kinetic model	General Equation	Linear Equation	Plot
First-order	$C_t = C_o e^{-k_1 t}$	$ln[C_t] = ln[C_o] - k_1 t$	$ln[C_t]\ vs.\ t$
Second-order	$C_t = \frac{C_0}{1 + C_0 k_2 t}$	$\frac{1}{C_t} = \frac{1}{C_0} + k_2 t$	$\frac{1}{C_t}\ vs.\ t$

Table 3: Equilibrium isotherm model equations for batch sorption experiments

Kinetic Model	Equation	Linear Equation	Plot
Langmuir	$q_e = Q_{max}\left[\frac{bC_e}{1 + bC_e}\right]$	$\left(\frac{C_e}{q_e}\right) = \left(\frac{1}{bQ_{max}}\right) + \left(\frac{1}{Q_{max}}\right) C_e$	C_e/q_e vs. C_e
Freundlich	$q_e = K_f {C_e}^{1/n}$	$Log(q_e) = Log(K_f) + \frac{1}{n} Log(C_e)$	$Log(q_e)$ vs. $Log(C_e)$

3.3 Mini Column Experiments

Miniature flow-through column experiments were designed based on previous work by Dittrich *et al*. and were used to better understand partitioning of Nd with the variable IS (0.1 and 5.0 M) and pH conditions as described above for batch experiments (Dittrich and Reimus, 2015; Dittrich et al., 2016). Columns are 1 cm in length with a porosity of approximately 0.3 and pore volume of approximately 0.4 mL as determined by mass. The flow rate is 1.5 mL/hr (36 mL/day) for all columns which is equivalent to a 17.5 minute retention time within the columns.

3.3.1 Preconditioning Columns

Preconditioning of the columns was done to equilibrate the mineral to the desired pH. The feed solution was pumped into the columns from the bottom to avoid introduction of air bubbles and gravity effects. Effluent was collected and analyzed for pH and major cations (Ca, Mg, Na) and aqueous carbonate by ICP-MS. Once the effluent pH reached that of the injection pH, then the column is pre-equilibrated and ready for the next step.

3.3.2 Sorption Experimental Procedure

Once the preconditioning of the column is complete, Nd was injected into the column from the bottom in the presence of the chosen IS (NaCl + 3 mM $NaHCO_3$). The effluent was collected continuously and analyzed at regular intervals (every 240 minutes) for Nd via ICP-MS following acidification in 2% HNO_3. Select samples were also analyzed for major cations and filtered to check for particulate versus dissolved phases. This phase of the experiment will be terminated once the effluent contaminant concentration reaches the influent concentration (i.e., the column has been saturated with respect to the contaminant of concern and available sorption sites on the dolomite mineral). However, columns are still ongoing due to the high sorption capacity of dolomite for Nd.

3.3.3 Desorption Experimental Procedure

After the adsorption phase is complete, desorption of Nd will be studied by pumping pH-adjusted solutions without the contaminant of concern through the columns or by a batch leaching setup. For the column procedure, effluent samples will be collected at regular intervals until the pH of the effluent solution reaches the pH of the inlet solution. In order to conduct mass balance calculations, a final desorption step may be conducted by transferring the column material into a centrifuge tube with HNO_3 (pH 2-3). The concentration of the contaminant desorbed by acid will be measured by ICP-MS as described above.

3.3.4 Retardation Factor Calculations

The potential for transport of the contaminant of concern will be quantified by calculating a retardation factor (R). A retardation factor is the ratio of the average linear velocity of groundwater to the velocity of the contaminant. Therefore, a conservative tracer should have a retardation factor of 1.0, but a contaminant that transports more slowly through a system than the tracer will have a retardation factor greater than 1.0. The retardation factor is estimated based on the mean residence time τ (Eqn. 5) and can be expressed in terms of the aqueous volume V (Eqn. 6) (Clark, 1996). The final retardation factor is calculated by dividing the aqueous volume, V_{aqu}, by the pore volume, V_{pore}, of the column. The pore volume is estimated for each column based on the difference in the dry, packed column mass and the wet column mass. The retardation factor (R) can be related to K_d by Eqn. 7 below. The ρ_b represents the bulk density of the mineral or sediment and n_e represents the effective porosity. In this manner, batch and column K_ds can be easily compared. Although the column experiments have not yet reached saturation, retardation factors are presented below based

on batch experiments. Once columns have sufficient breakthrough, a retardation factor will be calculated.

$$\tau = \frac{\int tC(t)dt}{\int C(t)dt} \quad \text{Eqn. 5}$$

$$V_{aqu} = \frac{\int VC(t)dV}{\int C(t)dV} - \frac{V_{spike}}{2} \quad \text{Eqn. 6}$$

$$R = 1 + \frac{K_d \times \rho_b}{n_e} \quad \text{Eqn. 7}$$

3.4 Instrumentation, Chemicals and Reagents

The following instruments and equipment are being during the experiments and analysis:

- Soil characterization materials:
  - Fisher stainless steel sieve [No. 45, 100, 200 and pan]
  - Chempex Impact mortar and pestle, stainless steel [Cat. No. 850]
- pH electrode and meter [Thermo Scientific Orion Star A211 meter and Orion 9156BNWP electrode]
- Culebra dolomite (collected by Timothy Dittrich from WIPP)
- Equipment
  - Syringe pump [Kd Scientific Model 100 series or Kloehn]
  - Fraction collector [Gilson FC203B or Eldex universal fraction collector]
  - Inductively Coupled Plasma Mass Spectrometer (ICP-MS) [Agilent 7900]
  - Inductively Coupled Plasma Optical Emission Spectrometer (ICP-OES) [Perkin Elmer Optima 7300 DV]
- Column materials
  - 1/8” 27 NPT carbon pipe tap [Drillco cutting tools, 2700E108]
  - 1/8” Teflon fitting [Ipolymer, MCF12]
  - Teflon tubing [thin wall natural, PTFE#20, Item# 06417-31]
  - 35 µm PEEK screen
  - 20 gauge Teflon tubing
  - 3-way luer lock
  - Polypropylene syringe (for Kd pump) or Glass syringe with Teflon fittings (for Kloehn pump)

- Silicone adhesive and Loctite marine epoxy (for column)

- Chemicals and Reagents
  - HCl, HNO_3 and NaOH, ACS reagent grade
  - NaCl, ACS reagent grade
  - $MgCl_2$, ACS reagent grade
  - Nd(III), Pu(III), and Am(III) stock solutions (Nd from High Purity Standards)

4.0 Results

4.1 Dolomite Mineral Characterization

The Culebra sample (355 – 500 µm size fraction) was consistent with the dolomite mineral [$CaMg(CO_3)_2$] based on XRD and SEM-EDX as shown in Figure 1 and Figure 2. Further, EDS analysis did not show significant impurities although analysis of more locations may be required to be statistically significant. BET surface area was measured at 1.70 m^2/g.

Element	Wt%	At%
CK	10.55	19.97
OK	28.08	39.92
MgK	14.35	13.43
CaK	47.02	26.68

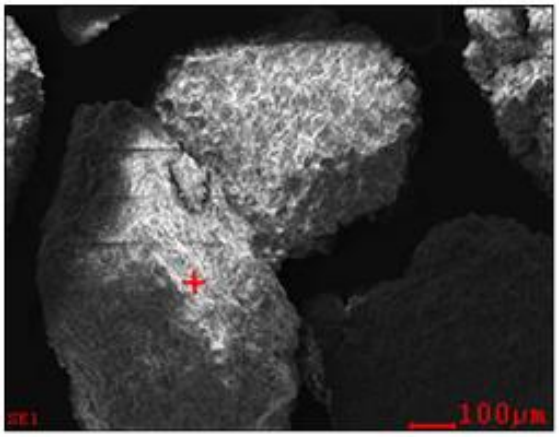

Figure 1: Representative SEM EDX analysis of Culebra formation, 355-500 µm size fraction, consistent with dolomite.

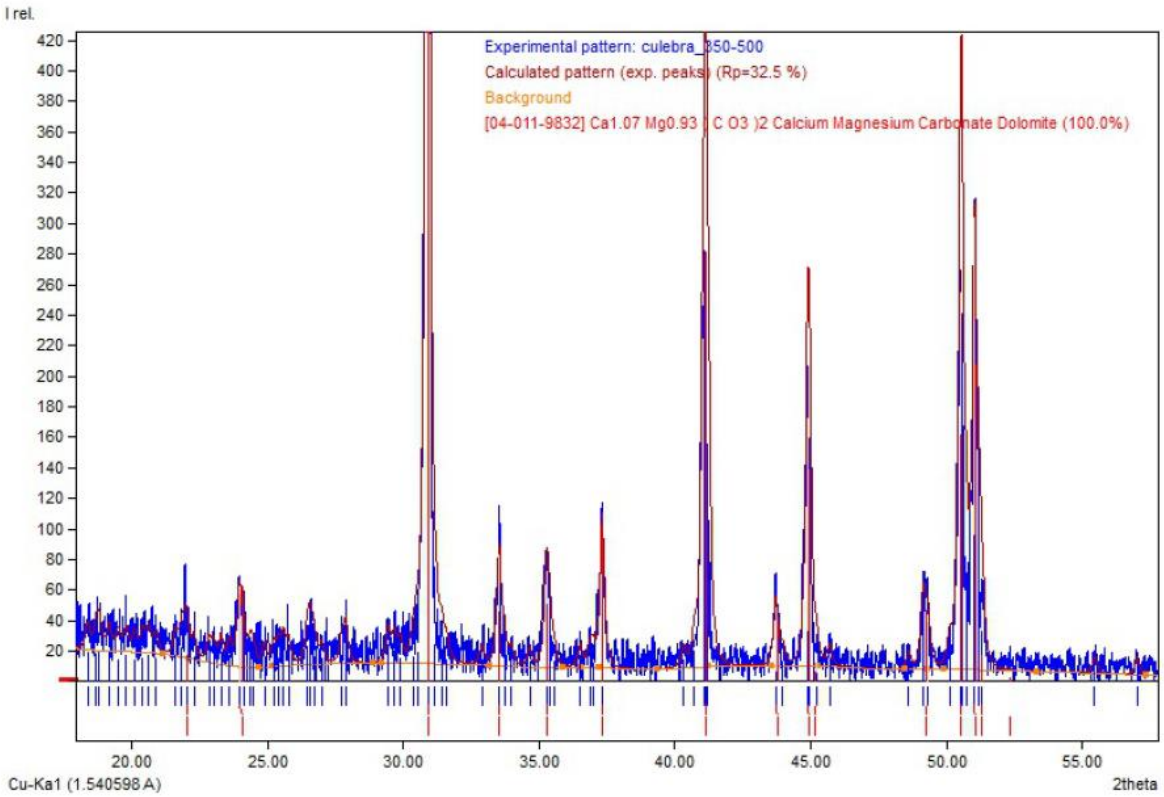

Figure 2: XRD spectra with reference spectra from Culebra formation, 355-500 µm size fraction for dolomite (Match! Software).

4.2 Batch Kinetics Results

Batch kinetics experiments were completed at 0.01 to 5.0 M total IS (3 mM $NaHCO_3$ + NaCl), and 0.5, 1.0 and 5.0 g/L dolomite in the presence of 20 ppb Nd. Figure 3 represents sorption with respect to time in terms of the fraction remaining in the aqueous phase for the 2.0 M IS experiments while a partitioning coefficient (K_d in mL/g) is calculated for comparison in Figure 4. Figure 5 shows results of kinetics experiments for all ISs up to 300 minutes. Samples were collected up to 3 days (4,320 minutes). However, data shows that sorption is strong and fast with equilibrium reached by 24 hours.

Equilibrium K_d's are measured between 500 – 6400 mL/g with increasing sorption with increasing IS as shown in Table 4. Further, it should be noted that kinetics are similar for each of the different IS although measurement error increases significantly after 24 hours. The increase in error after 24 hours may indicate a surface precipitation or incorporation process. However, measurements are also below limits of detection (LOD) for the higher IS (> 2 M after 300 minutes) samples because a significant dilution was required to avoid issues with the ICP-MS and due to low concentrations in the aqueous phase.

Table 4 also shows the equilibrium pH and pC_{H+} as determined using the corrections based on equation 1 and 2 in the Materials and Methods section developed previously (Borkowski et al., 2009). Although propagation of error from the linear fit significantly increased the error of the pC_{H+}, measurements are consistent across ionic strength. This stability indicates that the corrections for hydrogen ion activity outlined in the experimental methods above are appropriate for converting the hydronium concentration at high ionic strength.

Table 4: Summary of pH, pC_H, and K_d coefficients at 24 hours for variable ionic strength (3 mM $NaHCO_3$ + NaCl) batch experiments

	pH	pC_{H+}	K_d (mL/g)	K_d (m^2/g)
5.0 M	7.42±0.11	8.28±0.38	6380±3060	3750±1800
2.0 M	7.92±0.23	8.22±0.43	1180±450	695±262
1.0 M	8.29±0.08	8.41±0.38	819±225	482±132
0.1 M	8.64±0.08	8.59±0.38	724±105	426±62
0.01 M	8.67±0.11	8.60±0.39	503±129	296±76

Note: pC_{H+} corrections based on Borkowski *et al.,* 2009 with error propagated from their fit with a linear model

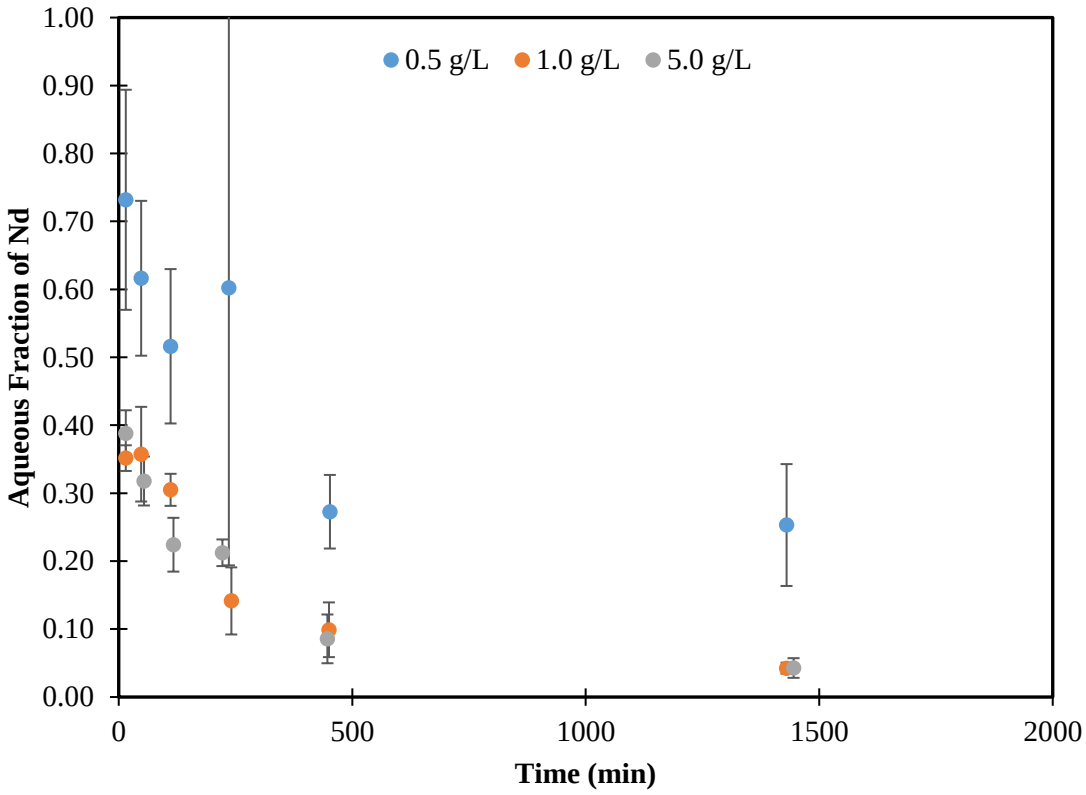

Figure 3: Aqueous fraction remaining of initially 20 ppb Nd batch reactors in the presence of 0.1, 0.5 and 5 g/L dolomite with respect to time in 2.0 M total ionic strength (NaCl + 3 mM $NaHCO_3$), Note: error bars represent the error for triplicate samples.

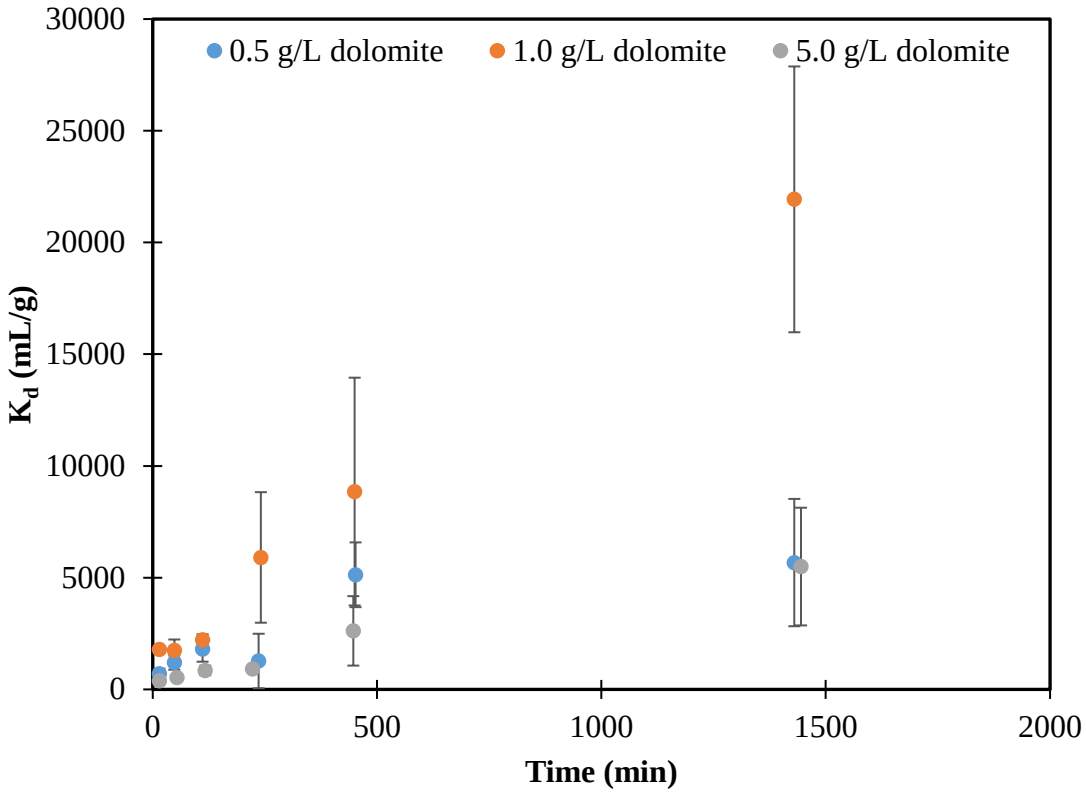

Figure 4: Partitioning coefficient (K_d, mL/g) for initially 20 ppb Nd in batch reactors in the presence of 0.1, 0.5 and 5 g/L dolomite with respect to time in 2.0 M total ionic strength (NaCl + 3 mM $NaHCO_3$), Note: error bars represent the error for triplicate samples.

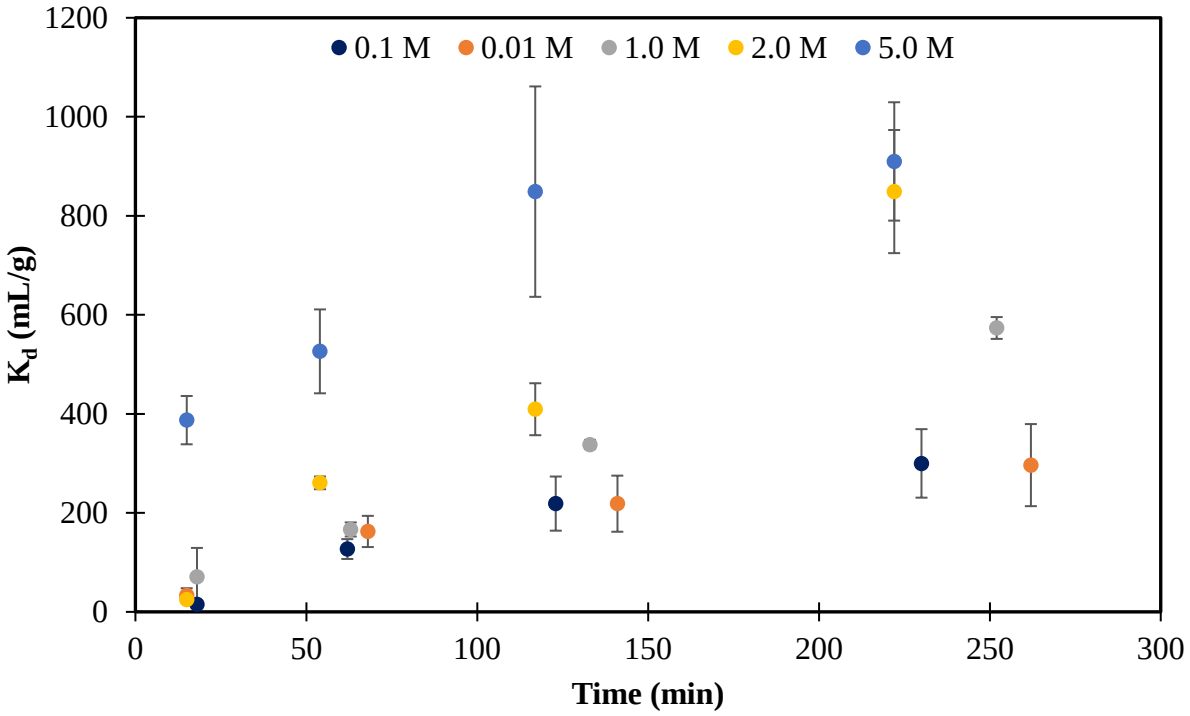

Figure 5: K_d (mL/g) partitioning of 20 ppb Nd in the presence of 5 g/L dolomite with respect to time in 0.01, 0.1, 1.0, 2.0 and 5.0 M total ionic strength (NaCl + 3 mM $NaHCO_3$), Note: error bars represent the error for triplicate samples.

4.3 Mini Column Breakthrough

Long-term mini columns with 0.1 or 5.0 M total IS (3 mM $NaHCO_3$ + NaCl) and 20 ppb Nd continuous injection at 1.5 mL/hr are currently in progress (Figure 6 and Figure 7). More than 15,000 pore volumes (6 months of continuous injection) have been pushed through the columns without saturation. However, the columns are nearing saturation as breakthrough has reached approximately 30% of the initial input. It is notable that the breakthrough curves for both 0.1 and 5.0 M total IS are not significantly different as the batch kinetics experiments reached significantly different levels of removal depending on IS. Possible theories for these disagreements are explored below in the discussion section.

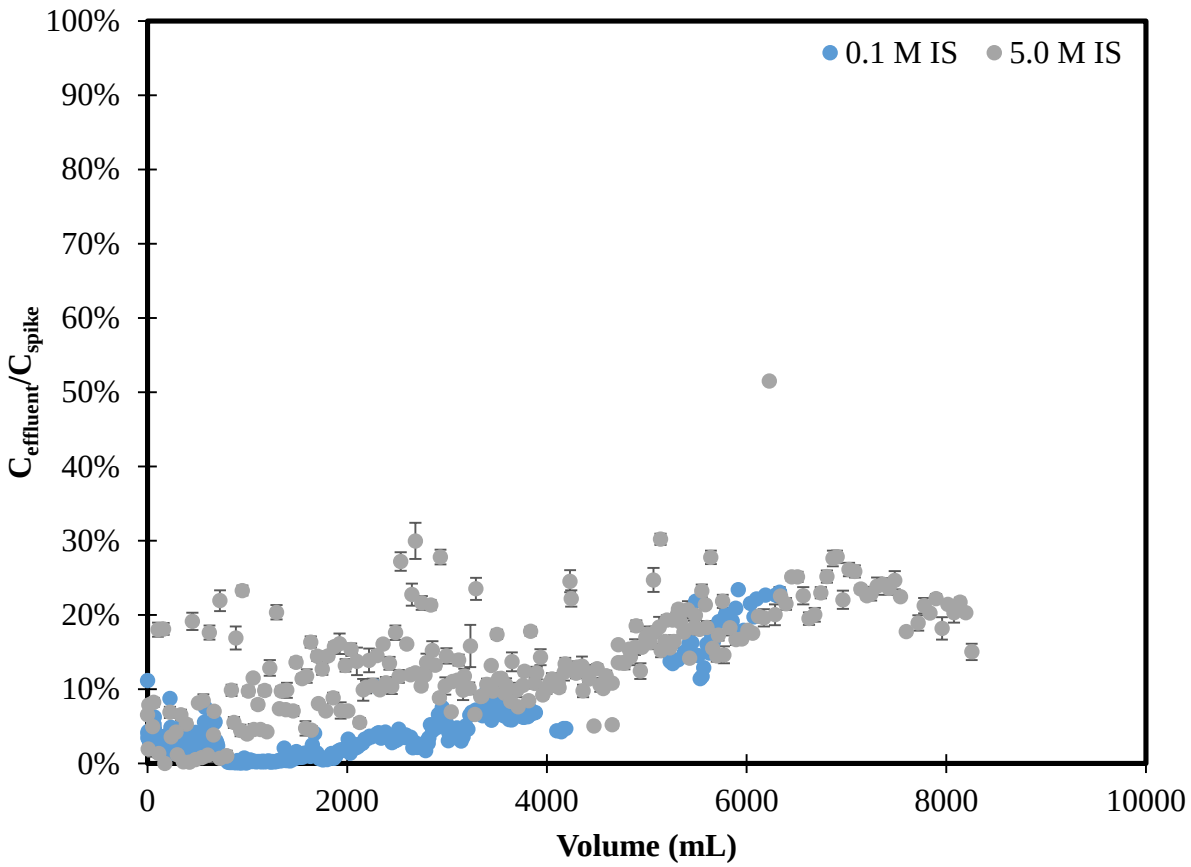

Figure 6: Effluent Nd breakthrough with respect to total injection volume for 0.1 (blue) and 5.0 M (gray) ionic strength (3 mM $NaHCO_3$ + NaCl) with continuous injection of 20 ppb Nd at 1.5 mL/hr, Note: error bars represent the error on triplicate analysis of individual samples by ICP-MS.

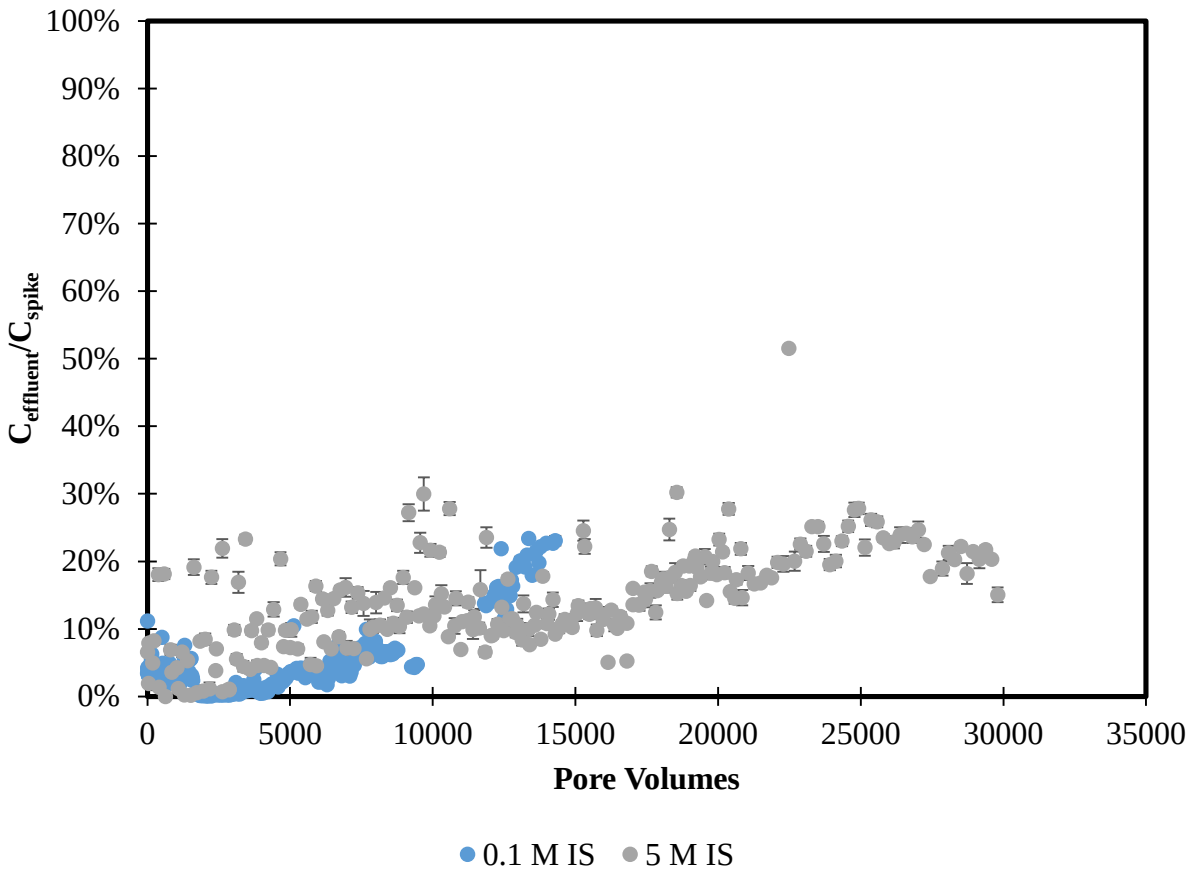

Figure 7: Effluent Nd breakthrough with respect to pore volumes for 0.1 (blue) and 5.0 M (gray) ionic strength (3 mM $NaHCO_3$ + NaCl) with continuous injection of 20 ppb Nd at 1.5 mL/hr, Note: the error bars represent the error based on triplicate analysis of individual samples by ICP-MS.

5.0 Discussion

5.1 Comparison of variable IS batch experiments with previous literature

The equilibrium K_d values measured for removal of 20 ppb Nd with 5 g/L dolomite suspensions was 6380 ± 3060 mL/g at 5.0 M IS versus 503 ± 129 mL/g at the lowest IS studied, 0.01 M (Table 4). Although the error is large on high IS measurements, due to the significant dilution required for measurement on ICP-MS and the low aqueous concentrations of Nd, there is a clear trend showing an increase in K_d with respect to IS in the batch experiments. However, previous experiments have reported varying effects of IS on sorption.

Previous work has produced varying results including: (1) no effect of IS (Brady et al., 1999; Schnurr et al., 2015), (2) a decrease in sorption with IS (Powell, 2016), and (3) an increase in sorption with IS (Ams et al., 2013; Powell, 2016). Brady and team may not have observed an effect of IS on sorption of Nd and Am to dolomite because of the low range of IS (up to 0.5 M) in their experiments as compared to the current work (Brady et al., 1999). However, experiments by Schnurr *et al*. considered sorption of Eu above pH 8 to natural clay samples up to 4.37 m IS without observing an effect of IS (Schnurr et al., 2015).

A decrease in sorption with respect to IS may be observed if removal is due to ion exchange as the salts in suspension can compete with actinides and lanthanides for ion exchange sites. However, the ionic radii of Na^{+} versus Nd^{+3} and Am^{+3} in solution are quite different as discussed below, so competition for exchange sites is not expected. Furthermore, it is more likely that surface complexation processes are the dominant sorption reactions in this system. Surface complexation processes generally dominate at neutral to basic pH over ion exchange for trivalent actinides and lanthanides as observed for Eu on clays (Bradbury and Baeyens, 2002), and dolomite is not expected to have a significant cation exchange capacity based on its structure.

Mancinelli and team have shown that the hydration of Na^{+} remains fairly constant (4.5 – 5.3) across the range of IS in this study with a slight trend to decrease with increasing IS (

Table 5) (Mancinelli et al., 2007). Therefore, with a coordination number of 4 – 5, the ionic radii in aqueous solutions for Na^{+} is 0.99 – 1.0 pm based on previous measurements (Shannon, 1976). The coordination number for trivalent actinides and lanthanides in water has been reported at 8 – 9, with a decreasing trend across each series (Rizkalla and Choppin, 1994). Although, recent EXAFS and modeling indicate that 9 may be the most likely coordination number for trivalent actinides and lanthanides across the series (D'Angelo et al., 2013). For a hydration of 8 – 9 water molecules, the ionic radii of Am^{3+} is 1.09 – 1.22 and for Nd^{3+} is 1.109 – 1.163 (D'Angelo et al., 2013; Shannon, 1976). Therefore, the ionic radii of Am^{3+} and Nd^{3+} versus Na^{+} is at least 10% greater under the conditions of these experiments.

Table 5: Number of H_2O molecules coordinated with Na+ in aqueous solutions at variable ionic strength (Mancinelli et al., 2007)

Molar/Atom Ratio NaCl:H_2O	Concentration NaCl (mol/L)	NaO (CN)
1:83	0.66	5.3±0.8
1:40	1.34	5.1±0.9
1:17	3.00	4.6±1.4
1:10	4.83	4.5±1.4

An increase in removal of the contaminant with respect to IS may be due to two different mechanisms: (1) the effects of increasing IS on ion activity and speciation (Ams et al., 2013; Sø et al., 2011) or (2) the effects of increasing IS on mineral dissolution and contaminant removal through incorporation and surface precipitation. Ams and team previously reported that the increase in ion activity led to an increase in hydrolysis and carbonate complexation constants for 2 and 4 M IS (Ams et al., 2013). This increase in hydrolysis species for Np(V) was hypothesized to lead to an increase in sorption to microbes based on the increased sorption affinity of these species. Similar conclusions were reached previously for phosphate sorption to calcite with surface complexation modeling (Sø et al., 2011). However, it must be noted that it is unlikely that Cl^- complexation of the trivalent lanthanides and actinides will be significant as previous work did not observe significant inner sphere complexation until greater than 6 M HCl for lanthanides (Yaita et al., 1999) and 8 M LiCl for both actinides and lanthanides (Allen et al., 2000). Furthermore, Allen *et al*. concluded that outer sphere sorption is the only manner in which Cl^- complexation could occur below 5 M IS.

In the dolomite batch experiments, FIU hypothesizes that the surface incorporation and precipitation is the dominant process leading to an increase in removal at greater IS based on the current system with support from previous work. In general, the carbonate minerals exhibit greater reactivity and dissolution than oxide and silicate minerals (Morse and Arvidson, 2002). Moreover, the dissolution rate of minerals that produce charged ions [like dolomite, $CaMg(CO_3)_2$] increases with IS due to a decrease in activity coefficients as shown theoretically in Figure 8 and

experimentally in Figure 9 (Langmuir, 1997; Pokrovsky et al., 1999). Based on this increased dissolution as IS increased, FIU expects greater surface precipitation and incorporation of Nd over time.

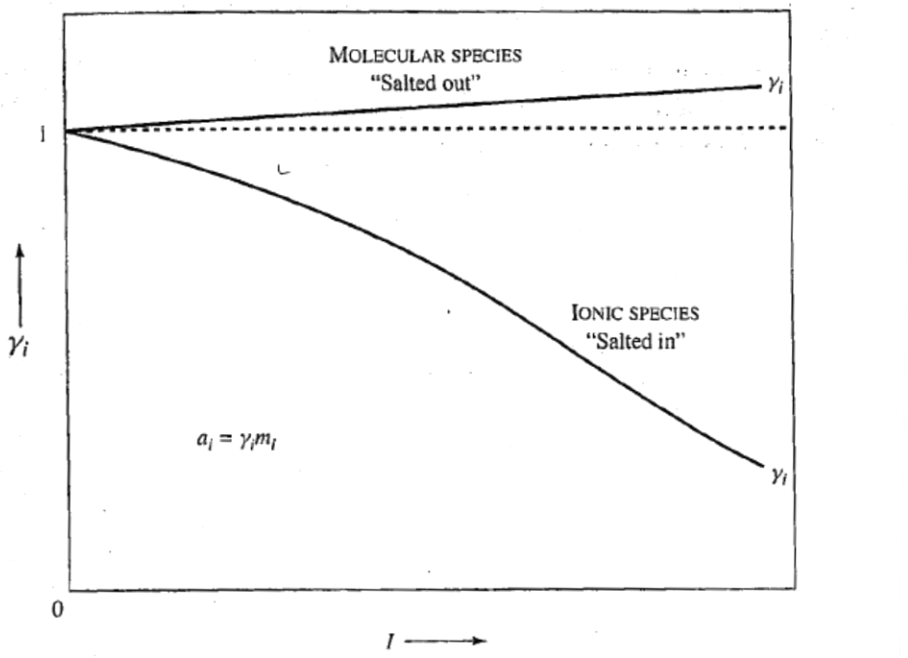

Figure 8: Plot representing the theoretical "salting in" γ < 1 and "salting out" γ > 1 behavior of ionic and molecular species, respectively (Langmuir, 1997).

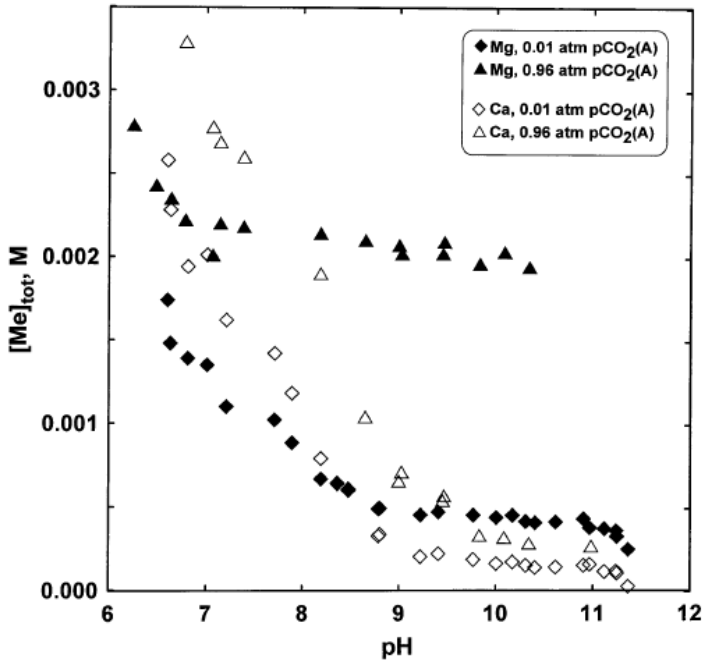

Figure 9: pH dependence of total Ca and Mg concentrations in stirred reactor suspension at variable ionic strength and atmospheric CO_2 as determined previously (Pokrovsky et al., 1999).

Coupled substitution of Na^+ and Am/Nd^{3+} with Ca^{2+} and Mg^{2+} in the dolomite mineral or secondary precipitates such as calcite would lead to increasing incorporation of Nd with increasing ionic strength. Previous analysis by Dawson on natural carbonatite samples containing dolomite and calcite from Phalaborwa, South Africa, showed that these elements can be incorporated into carbonate minerals. Furthermore, they observe some important trends in actinide and lanthanide partitioning in these minerals (Dawson and Hinton, 2003): (1) significant concentrations of lanthanides and actinides are reported as shown in Table 6, (2) greater concentrations of actinides and lanthanides are observed in calcite as compared to dolomite, and (3) Na concentrations are correlated with all rare earth element concentrations with 1.5 – 3.0 times more Na than required for coupled substitution.

Table 6: Na, Nd, Eu, Th and U content in ppm in natural calcite and dolomite minerals from Phalaborwa, South Africa as determined by electron probe (Dawson and Hinton, 2003)

Element	Calcite	Dolomite
Na	627	125
Nd	405	84
Eu	18.3	3.38
Th	0.02	-
U	-	0.01

Previous TRLFS measurements provide additional confirmation of the likelihood of incorporation in a laboratory setting with observation of two surface species for Cm^{3+} interacted with calcite including: (1) a surface adsorbed species and (2) an incorporated species at pH 8.1 at 0.01 M IS (as $NaClO_4$) (Fernandes et al., 2008). Further, sorption of Am on calcite was previously found to be largely irreversible, suggesting surface precipitation (Higgo and Rees, 1986; Shanbhag and Morse, 1982). Therefore, it is likely that both sorption and incorporation (potentially as a coupled substitution) processes are occurring in the current batch experiments.

5.2 Comparison of batch and mini column experimental results

The preliminary results for the mini column experiments do not show a difference in removal of Nd with respect to ionic strength in direct contrast with the batch experiments. However, the conditions are quite different due to the presence and absence of flow in column versus batch, respectively. The working hypothesis is that the mini column experiments do not have a long enough reaction time for the surface precipitation and incorporation processes described above to occur. Therefore, the mini column experiments are dominated by removal of Nd through sorption while the batch experiments are a combination of sorption and incorporation processes.

Because of the short (17.5 minute) retention time of the solutions within the mini columns, there is not sufficient time for mineral dissolution and re-precipitation processes to remove Nd from the aqueous phase. For example, the rate of dolomite dissolution at neutral pH is on the order of 5 x 10^{-12} mol/sec/cm^2 based on the review of carbonate mineral dissolution by Morse (Morse and Arvidson, 2002). Therefore, FIU hypothesizes that there is not sufficient time for Ca/Mg to dissolve from the dolomite in sufficient concentrations to re-precipitate. Previous work by Brady et al. supports this theory as an effect of IS was not observed up to 0.5 M likely because of the short (30 second) reaction time (Brady et al., 1999).

Furthermore, because of the increased reaction time of the aqueous phase with the dolomite mineral in batch experiments, there is time for dissolution and re-precipitation processes to affect Nd removal from the aqueous phase. This is supported by measurements of Ca^{2+} and Mg^{2+} in the aqueous phase for both batch and mini column experiments as shown for the 5.0 M IS samples in Table 7 below. The Ca^{2+} and Mg^{2+} concentrations are nearly double in the batch experiments as compared to the mini columns, indicating greater dissolution of the minerals and likely greater re-precipitation over time.

Table 7: Aqueous Ca and Mg in 5.0 M ionic strength batch and mini column experiments for select samples as analyzed by ICP-OES

Experiment	Ca (µM)	Mg (µM)
Batch	184±85	72±11
Column	103±2	30±5

5.3 Remediation Relevance

Although experiments are still ongoing, significant improvements to the experimental methodology have been made as compared to previous work conducted in the 1990's. Previous work reported sorption K_ds on the order of $10^{3.4}$ to 10^6 (Brady et al., 1999; Brush and Storz, 1996; Perkins et al., 1999). However, these experiments were limited in pH range and IS conditions evaluated and had precipitation and solubility issues. Therefore, the values reported in this work are expected to be more representative.

Preliminary results show that sorption of Nd is likely greater than was assumed in the performance assessment process for the WIPP. The performance assessment models assumed a K_d of 20 – 400 mL/g (Brush and Storz, 1996). The current preliminary batch experiments predict sorption K_ds of 500 – 6400 mL/g with the highest equilibrium K_d being most representative as it was measured at 5 M IS. The preliminary values in this work show that the initial performance assessment models may have been conservative and likely overpredict transport of the trivalent actinides and lanthanides.

Once breakthrough is achieved for the mini column experiments, this will provide a unique opportunity to compare both batch sorption and column experiments. This is an important endeavor as each of the types of experiments induce different experimental artifacts. In addition, this is the first dataset known to the author of this report that investigates the kinetics of sorption of Nd to dolomite at variable ISs. This will provide a better basic understanding of the effect of IS on sorption of Nd as well as an idea of the kinetics of sorption to indicate whether kinetic models (as opposed to equilibrium K_d models) are necessary for the performance assessment process for the WIPP.

6.0 Future Work

Future experiments will finalize kinetic and equilibrium sorption parameters for Nd in order to provide guidance in updating performance assessment models for the five year re-certification of the WIPP.

1. All batch kinetics data will be fit with common kinetic and equilibrium sorption models as described in the methodology section.

2. The long-term mini columns at 0.1 and 5.0 M total IS will be stopped after breakthrough (i.e. saturation) has been reached, although desorption experiments may be considered for future work as described above.
3. A model will be developed to describe the column breakthrough data utilizing PHREEQC.

Furthermore, experiments will endeavor to confirm that sorption processes are dominant in mini column experiments while sorption and incorporation occur in batch experiments. These results will significantly affect the experimental design for future work pertaining to contaminant interactions with carbonate minerals as adjustments may be necessary to target specific processes. A portion of dolomite from each of the column and batch experiments will be removed and analyzed via TEM or SEM-EDS to compare adsorption (to the surface) versus incorporation into dolomite minerals. Microscopy samples will be prepared in epoxy and either polished (for SEM) or thin sections will be prepared with a microtome (for TEM) to investigate the depth to which Nd has moved into particles in both experiments in order to confirm sorption to the surface or incorporation processes.

References

Allen, P., Bucher, J., Shuh, D., Edelstein, N., Craig, I., 2000. Coordination chemistry of trivalent lanthanide and actinide ions in dilute and concentrated chloride solutions. Inorganic chemistry 39, 595-601.

Ams, D.A., Swanson, J.S., Szymanowski, J.E., Fein, J.B., Richmann, M., Reed, D.T., 2013. The effect of high ionic strength on neptunium (V) adsorption to a halophilic bacterium. Geochimica et Cosmochimica Acta 110, 45-57.

Bertram-Howery, S.G., Marietta, M.G., Rechard, R.P., Swift, P., Anderson, D., Baker, B., Bean Jr, J., Beyeler, W., Brinster, K., Guzowski, R., 1990. Preliminary comparison with 40 CFR part 191, subpart B for the Waste Isolation Pilot Plant, December 1990. SAND90-2347. Sandia National Laboratories, Albuquerque, New Mexico.

Borkowski, M., Lucchini, J.F., Richmann, M., Reed, D., 2009. Actinide (III) Solubility in WIPP Brine: Data Summary and Recommendations, in: Laboratory, L.A.N. (Ed.).

Bradbury, M., Baeyens, B., 2002. Sorption of Eu on Na-and Ca-montmorillonites: experimental investigations and modelling with cation exchange and surface complexation. Geochimica et Cosmochimica Acta 66, 2325-2334.

Brady, P.V., Papenguth, H.W., Kelly, J.W., 1999. Metal sorption to dolomite surfaces. Applied Geochemistry 14, 569-579.

Brush, L.H., Storz, L.J., 1996. Revised Ranges and Probability Distributions of Kds for Dissolved Pu, Am, U, Th, and Np in the Culebra for the PA Calculations to Support the WIPP CCA, in: Laboratories, S.N. (Ed.), Albuquerque, NM.

Chou, L., Garrels, R.M., Wollast, R., 1989. Comparative study of the kinetics and mechanisms of dissolution of carbonate minerals. Chemical Geology 78, 269-282.

Clark, M.M., 1996. Transport Modeling for Environmental Engineers and Scientists. John Wiley and Sons, New York, NY.

D'Angelo, P., Martelli, F., Spezia, R., Filipponi, A., Denecke, M.A., 2013. Hydration properties and ionic radii of actinide (III) ions in aqueous solution. Inorganic chemistry 52, 10318-10324.

Dawson, J., Hinton, R., 2003. Trace-element content and partitioning in calcite, dolomite and apatite in carbonatite, Phalaborwa, South Africa. Mineralogical Magazine 67, 921-930.

Dittrich, T.M., Reimus, P.W., 2015. Uranium transport in a crushed granodiorite: Experiments and reactive transport modeling. Journal of contaminant hydrology 175, 44-59.

Dittrich, T.M., Ware, S.D., Reimus, P.W., 2016. Mini-columns for Conducting Breakthrough Experiments: Design and Construction, in: Technologies, U.S.D.O.o.N.E.F.C. (Ed.). Los Alamos National Laboratory, Los Alamos, NM.

Fernandes, M.M., Stumpf, T., Rabung, T., Bosbach, D., Fanghänel, T., 2008. Incorporation of trivalent actinides into calcite: A time resolved laser fluorescence spectroscopy (TRLFS) study. Geochimica et Cosmochimica Acta 72, 464-474.

Higgo, J.J., Rees, L.V., 1986. Adsorption of actinides by marine sediments: effect of the sediment/seawater ratio on the measured distribution ratio. Environmental science & technology 20, 483-490.

Langmuir, D., 1997. Aqueous Environmental Geochemistry. Prentice Hall, Upper Saddle River, New Jersey.

Lucchini, J.F., Borkowski, M., Khaing, H.M., Richmann, M., Swanson, J.S., Simmona, K.A., Reed, D., 2014. WIPP Actinide-Relevant Brine Chemistry. Los Alamos National Laboratory, Carlsbad, NM.

Mancinelli, R., Botti, A., Bruni, F., Ricci, M., Soper, A., 2007. Hydration of sodium, potassium, and chloride ions in solution and the concept of structure maker/breaker. The Journal of Physical Chemistry B 111, 13570-13577.

Meigs, L.C., Beauheim, R.L., McCord, J.T., Tsang, Y.M., Haggerty, R., 1997. Design, modelling and current interpretations of the H-19 and H-11 tracer tests at the WIPP site, Field Tracer Experiments: Role in the Prediction of Radionuclide Migration. Nuclear Energy Agency, Cologne, Germany.

Morse, J.W., Arvidson, R.S., 2002. The dissolution kinetics of major sedimentary carbonate minerals. Earth-Science Reviews 58, 51-84.

Perkins, W.G., Lucero, D.A., Brown, G.O., 1999. Column Experiments for Radionuclide Adsorption Studies of the Culebra Dolomite: Retardation Parameter Estimation for Non-Eluted Actinide Species, in: Laboratories, S.N. (Ed.), Albuquerque, NM, p. 163.

Pokrovsky, O.S., Schott, J., Thomas, F., 1999. Dolomite surface speciation and reactivity in aquatic systems. Geochimica et Cosmochimica Acta 63, 3133-3143.

Powell, B., 2016. Quantification of Cation Sorption to Engineered Barrier Materials Under Extreme Conditions, Nuclear Energy University Programs Fuel Cycle Research and Development. Clemson University.

Rai, D., Felmy, A.R., Juracich, S.P., Rao, L.F., 1995. Estimating the Hydrogen Ion Concentration in Concentrated NaCl and Na2SO4 Electrolytes, in: Laboratories, S.N. (Ed.). Sandia National Lab, Albuquerque, NM.

Reeder, R., Wenk, H.-R., 1983. Structure refinements of some thermally disordered dolomites. American Mineralogist 68, 769-776.

Rizkalla, E.N., Choppin, G.R., 1994. Lanthanides and actinides hydration and hydrolysis. Handbook on the physics and chemistry of rare earths 18, 529-558.

Schnurr, A., Marsac, R., Rabung, T., Lützenkirchen, J., Geckeis, H., 2015. Sorption of Cm (III) and Eu (III) onto clay minerals under saline conditions: Batch adsorption, laser-fluorescence spectroscopy and modeling. Geochimica et Cosmochimica Acta 151, 192-202.

Shanbhag, P., Morse, J.W., 1982. Americium interaction with calcite and aragonite surfaces in seawater. Geochimica et Cosmochimica Acta 46, 241-246.

Shannon, R.t., 1976. Revised effective ionic radii and systematic studies of interatomic distances in halides and chalcogenides. Acta crystallographica section A: crystal physics, diffraction, theoretical and general crystallography 32, 751-767.

Sø, H.U., Postma, D., Jakobsen, R., Larsen, F., 2011. Sorption of phosphate onto calcite; results from batch experiments and surface complexation modeling. Geochimica et Cosmochimica Acta 75, 2911-2923.

Stout, D.L., Carroll, S.A., 1993. A literature review of actinide-carbonate mineral interactions. Sandia National Labs., Albuquerque, NM (United States).

Yaita, T., Narita, H., Suzuki, S., Tachimori, S., Motohashi, H., Shiwaku, H., 1999. Structural study of lanthanides (III) in aqueous nitrate and chloride solutions by EXAFS. Journal of radioanalytical and nuclear chemistry 239, 371-375.

Zavarin, M., Roberts, S.K., Hakem, N., Sawvel, A.M., Kersting, A.B., 2005. Eu(III), Sm(III), Np(V), Pu(V), and Pu(IV) sorption to calcite. Radiochimica Acta 93, 93-102.